

Supplementary Information for

Modeling the subsurface adsorption of atomic oxygen in silver from high vacuum to high pressure

Carson Mize^{a†}, Lonnie Crosby^{b†}, Elizabeth Lander^a, Sharani Roy^{*a}

^aDepartment of Chemistry, University of Tennessee, Knoxville, TN 37996, USA

^bNational Institute for Computational Sciences, University of Tennessee, Knoxville, TN 37996, USA

E-mail: sharani.roy@utk.edu

Equations to calculate the chemical potential (μ) of $O_2(g)$

For an ideal gas at pressure p , volume V , and temperature T , the equation of state is

$$pV = Nk_B T$$

The partition function for a harmonic oscillator-rigid rotor approximate model for the diatomic O_2 molecule (pg. 108, Eq. 6-51, "Statistical Mechanics", David McQuarrie, 2000) is

$$q(V, T) = \left(\frac{2\pi m_{O_2} k_B T}{h^2} \right)^{\frac{3}{2}} V \frac{8\pi^2 I k_B T}{\sigma h^2} e^{-\frac{h\nu}{2k_B T}} \left(1 - e^{-\frac{h\nu}{k_B T}} \right)^{-1} \omega_{e1} e^{\frac{D_e}{k_B T}}$$

where m_{O_2} , D_e , I , σ , ν , and ω_{e1} are mass, dissociation energy, moment of inertia, rotational degeneracy, vibrational frequency, and electronic degeneracy of O_2 , respectively, and h is the Planck constant. The chemical potential of this ideal gas is

$$\mu(p, T) = -k_B T \ln \frac{q(V, T)}{N}$$

Substituting gives

$$\frac{\mu(p, T)}{k_B T} = -\ln \left[\left(\frac{2\pi m_{O_2} k_B T}{h^2} \right)^{\frac{3}{2}} \frac{k_B T}{p} \right] - \ln \frac{8\pi^2 I k_B T}{\sigma h^2} + \frac{h\nu}{2k_B T} + \ln \left(1 - e^{-\frac{h\nu}{k_B T}} \right) - \frac{D_e}{k_B T} - \ln \omega_{e1}$$

The vibrational temperature ($\theta_v = \frac{h\nu}{k_B}$) and characteristic rotational temperature ($\theta_r = \frac{h^2}{8\pi^2 I k_B}$) hold for $\theta_r \ll T$. For O_2 , $\theta_v = 2256$ K and $\theta_r = 2.07$ K (pg. 95, Table 6-1, "Statistical Mechanics", David McQuarrie, 2000).

Substituting and labeling the translation, rotational, vibrational, and electronic contributions to the chemical potential:

$$\frac{\mu(p, T)}{k_B T} = \left\{ \begin{array}{llll} -\ln \left[\left(\frac{2\pi m_{O_2} k_B T}{h^2} \right)^{\frac{3}{2}} \frac{k_B T}{p} \right] & - \ln \frac{T}{\sigma \theta_r} & + \frac{\theta_v}{2T} & + \ln \left(1 - e^{-\frac{\theta_v}{T}} \right) & - \frac{D_e}{k_B T} & - \ln \omega_{e1} \\ \text{Trans.} & + \text{Rot.} & + \text{Vib.} & + \text{Elec.} & & \end{array} \right.$$

Since O_2 is a homonuclear diatomic molecule, $\sigma = 2$. The ground electronic state for O_2 is a triplet, therefore $\omega_{e1} = 3$. The dissociation energy including zero-point energy correction, D_0 , for O_2 is 118.0 kcal/mol (pg. 95, Table 6-1, "Statistical Mechanics", David McQuarrie, 2000). Adding in the zero-point energy, $ZPE = \frac{1}{2} k_B \theta_v$, the dissociation energy from minima of electronic energy, D_e , is 5.214 eV. m_{O_2} is 31.998 g/mol.

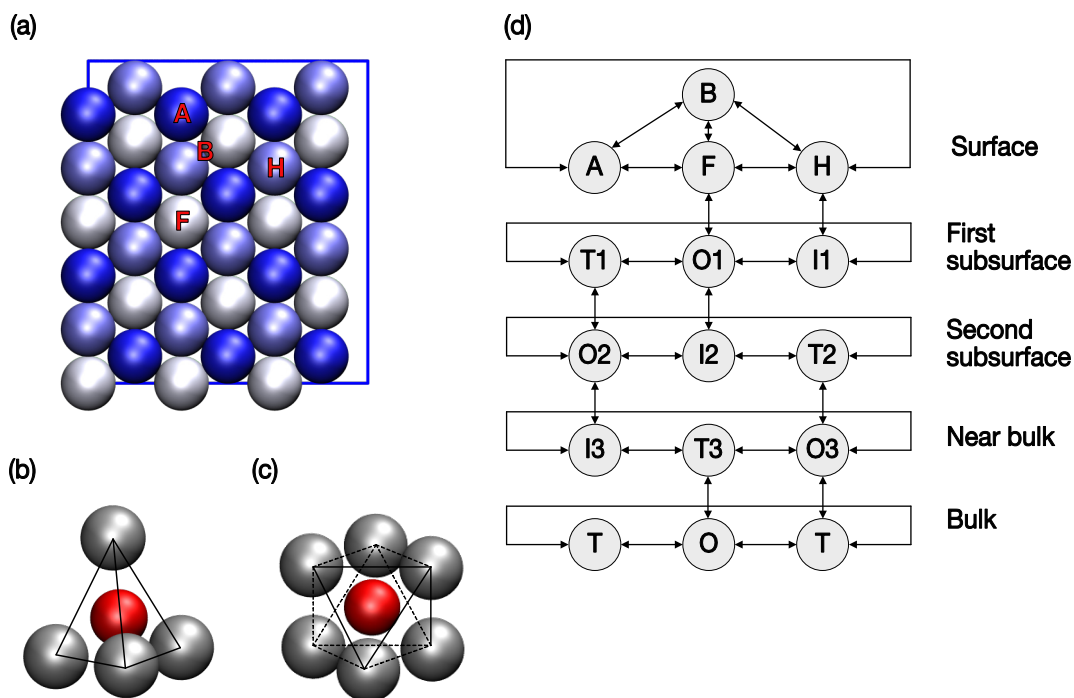


Fig. S1.

Binding sites on Ag(111): A = atop (surface), H = hexagonal close-packed (surface), F = face-centered cubic (surface), B = bridge (surface), T1 = tetrahedral (first subsurface), O1 = octahedral (first subsurface), I1 = inverted tetrahedral (first subsurface), T2 = tetrahedral (second subsurface), O2 = octahedral (second subsurface), I2 = inverted tetrahedral (second subsurface), T3 = tetrahedral (near bulk), O3 = octahedral (near bulk), I3 = inverted tetrahedral (near bulk), T = tetrahedral (bulk), O = octahedral (bulk). (A) Top view of the Ag(111) supercell showing the ABC stacking of atomic layers and binding sites on the surface. Dark blue = first Ag layer, light blue = second Ag layer, white = third Ag layer. (B) An O atom (red) surrounded by four Ag atoms (silver) in a tetrahedral site. In the analogous inverted tetrahedral site, the base of the Ag tetrahedron lies above the oxygen atom. (C) An O atom (red) surrounded by six Ag atoms (silver) in an octahedral site. (D) Connectivity map between binding sites at the surface, subsurface, near-bulk, and bulk regions of Ag(111).

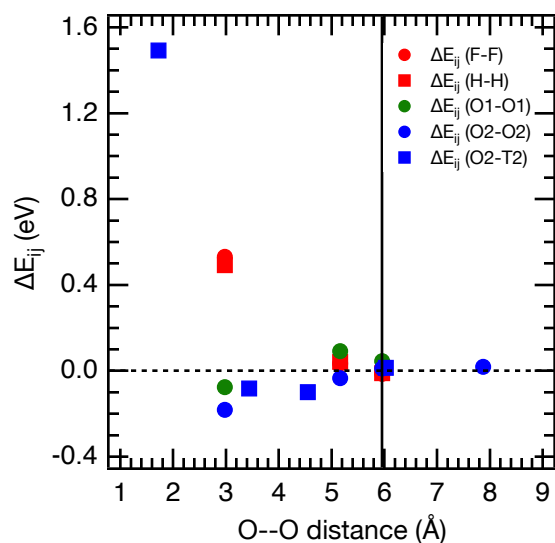


Fig. S2.

Pair interaction energies (ΔE_{ij}) as a function of O—O neighbor distance for F—F (red circles), H—H (red squares), O1—O1 (green circles), O2—O2 (blue circles), and O2—T2 (blue squares). The horizontal dashed black line demarcates $\Delta E_{ij} = 0$. The vertical solid black line demarcates the O—O cutoff distance of 5.98 Å. DFT tests of interaction energies at distances greater than the cutoff distance produced $\Delta E_{ij} = 0.019$ eV for the fourth-neighbor interaction across O2-O2 sites at 7.87 Å and $\Delta E_{ij} = 0.015$ eV for the fourth-neighbor interaction across O2-T2 sites at 6.02 Å.

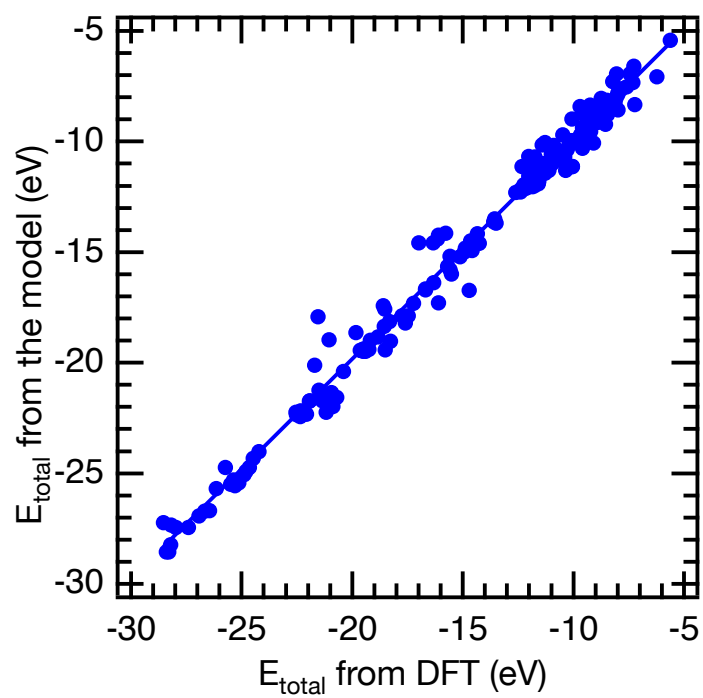


Fig. S3.

Parity plot comparing 219 DFT-computed total adsorption energies (E_{total}) of varying numbers of O atoms on Ag(111) to corresponding model energies. The linear-fit equation is $E_{\text{total,model}} = 0.073 + 0.994E_{\text{total,DFT}}$ with $R^2 = 0.989$. The RMSE is 0.646 eV.

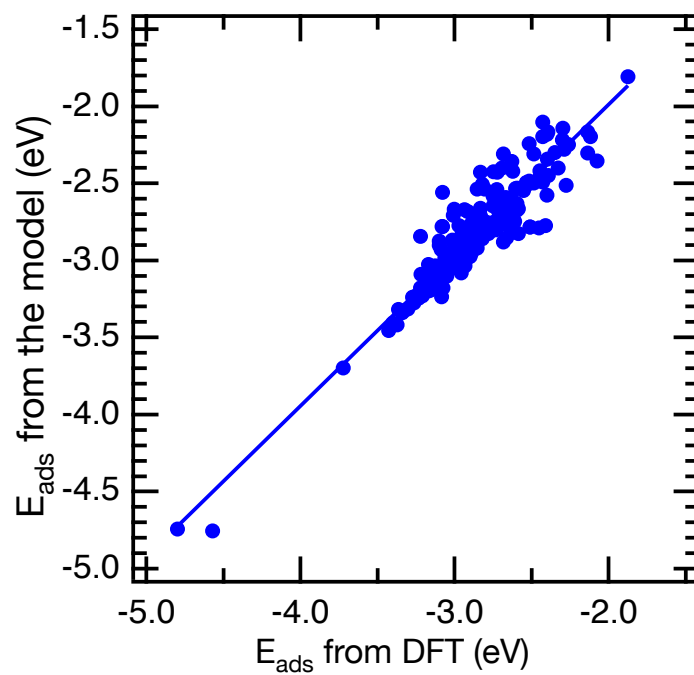


Fig. S4.

Parity plot comparing 219 DFT-computed average adsorption energies per O (E_{ads}) on Ag(111) to corresponding model energies. The linear-fit equation is $E_{\text{ads,model}} = -0.029 + 0.978E_{\text{ads,DFT}}$ with $R^2 = 0.872$. The RMSE is 0.132 eV.

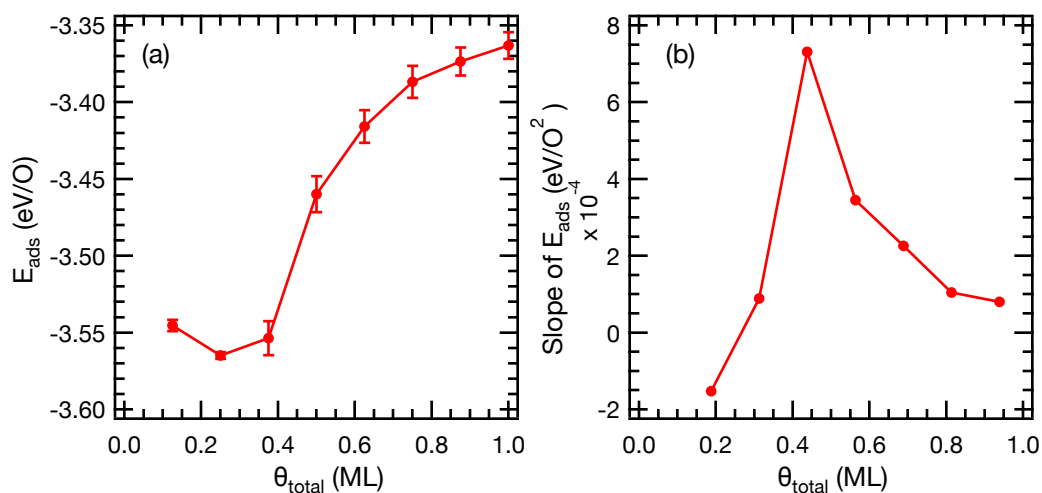


Fig. S5.

(a) Average adsorption energy per O (E_{ads}) and (b) slope of E_{ads} with respect to increase in oxygen atoms as functions of total oxygen coverage (θ_{total}) computed from canonical Monte Carlo simulations. As the average adsorption strength weakens sharply from θ_{total} of ~ 0.4 to 0.5 ML due to initial occupation of the subsurface, we chose initial configurations for the grand-canonical Monte Carlo simulations from converged canonical Monte Carlo distributions at $\theta_{\text{total}} = 0.75$ ML to ensure good sampling of subsurface oxygen coverages at all pressures and temperatures.

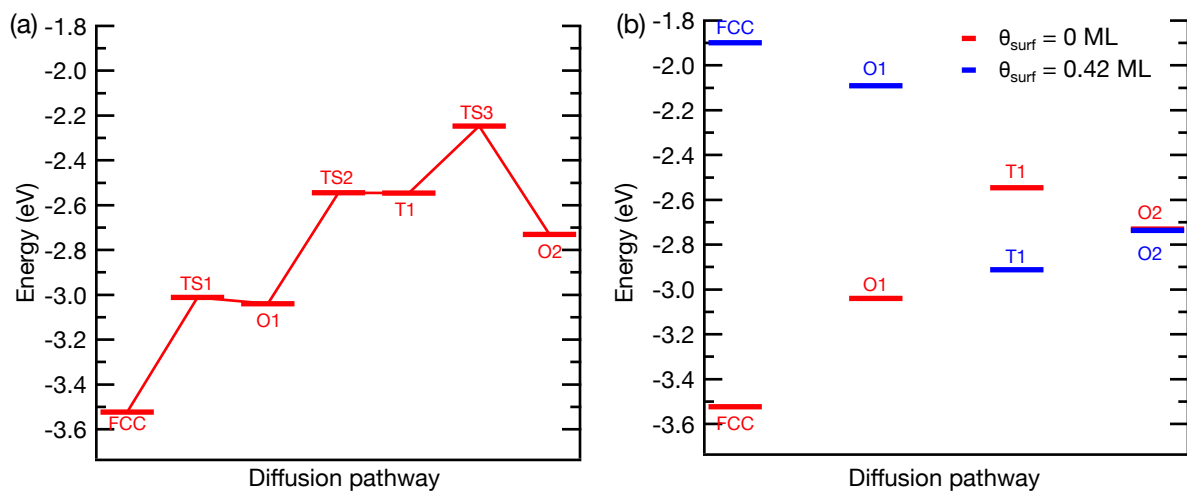


Fig. S6.

(a) DFT-computed pathway for surface-to-subsurface diffusion of an adsorbed O atom along the FCC → O1 → T1 → O2 sites of Ag(111) at $\theta_{\text{total}} = 0.08$ ML. Site definitions and connectivity are shown in Fig. S1. The energy is reported relative to the total adsorption energy of θ_{surf} , defined below. The “TS” labels indicate the transition states connecting the initial, intermediate, and final sites. (b) Comparison of adsorption energies of the diffusing oxygen atom at the four sites for $\theta_{\text{total}} = 0.08$ ML ($\theta_{\text{surf}} = 0$ ML), shown in red, and $\theta_{\text{total}} = 0.5$ ML ($\theta_{\text{surf}} = 0.42$ ML), shown in blue. θ_{surf} is the fixed oxygen coverage on the surface in addition to the diffusing oxygen atom. This fixed θ_{surf} occupies FCC and HCP sites on the surface. $\theta_{\text{surf}} = 0.42$ ML was chosen to represent the range of surface oxygen coverages (0.375 – 0.5 ML) in common O/Ag(111) reconstructions.

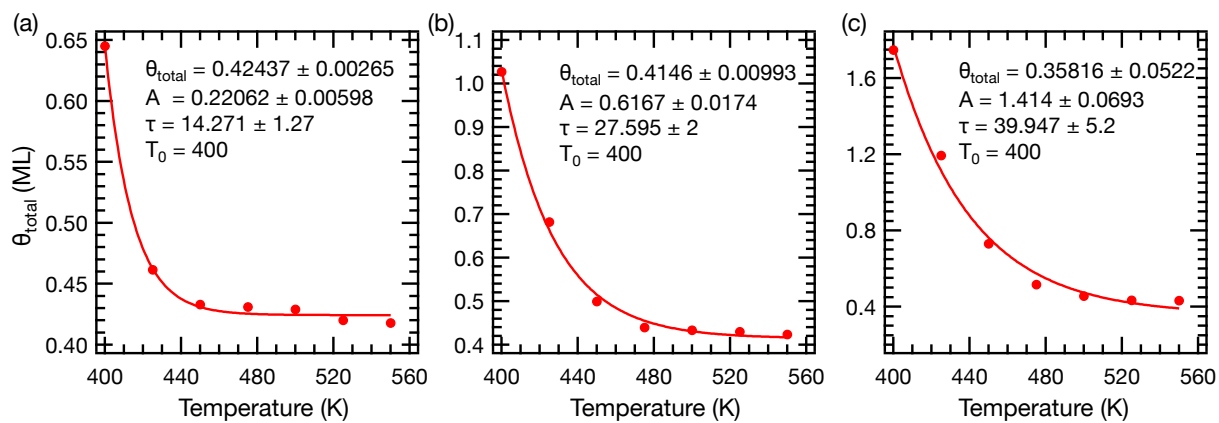


Fig. S7.

Fits of total oxygen coverage (θ_{total}) on or within the Ag(111) surface as a function of temperature for (a) $p_{O_2} = 0.01$ bar, (b) $p_{O_2} = 0.1$ bar, and (c) $p_{O_2} = 1$ bar. The fit equation is

$$\theta_{total} = \theta_0 + Ae^{\frac{-(T-T_0)}{\tau}}, \text{ where } T_0 \text{ is held constant in the fitting process.}$$

Table S1.

Adsorption energy (E_i) of an O atom adsorbed on the FCC hollow site, and the interaction energy (ΔE_{ij}) between two O atoms occupying first-neighbor FCC hollow sites on the Ag(111) surface as calculated using different PAW-PBE Version 54 pseudopotentials available in VASP (version 5.4). We used PAW-PBE energy cutoffs of 400 eV and 250 eV for O and Ag, respectively, to perform DFT calculations for the construction of our lattice-gas model.

PAW-PBE Energy Cutoff (eV)		E_i (eV)	ΔE_{ij} (eV)
O	Ag		
400	250	-3.523	0.341
700	250	-3.560	0.388
400	298	-3.503	0.342
700	298	-3.493	0.331

Table S2.

The RMSE of the model-derived energies compared to DFT within a fixed total oxygen coverage (θ_{total}). E_{total} is the total adsorption energy of the O atoms on Ag(111) and E_{ads} is the average adsorption energy per O atom on Ag(111). The “ALL” row shows the RMSE of energies over all calculated oxygen coverages. The RMSE of E_{total} in this row is shown in Fig. S2 and the RMSE of E_{ads} in this row is shown in Fig. S3.

θ_{total} (ML)	RMSE of E_{total} (eV)	RMSE of E_{ads} (eV)
ALL	0.646	0.132
3/12 = 0.250	0.401	0.134
4/12 = 0.333	0.569	0.142
5/12 = 0.417	0.497	0.091
6/12 = 0.500	0.876	0.146
7/12 = 0.583	1.027	0.147
8/12 = 0.667	0.546	0.068
9/12 = 0.750	0.542	0.060

Table S3.

Site-adsorption energies (E_i), vibrational frequencies, and free-energy corrections ($A_{i,corr}$) of an O atom bound to the FCC, HCP, O1 (octahedral in the first subsurface), and O2 (octahedral in the second subsurface) sites of Ag(111) at 298.15 K.

Adsorption site	E_i (eV)	Frequencies (cm ⁻¹)			$A_{i,corr}$ (eV)
FCC	-3.52	323.85	299.54	294.22	0.037
HCP	-3.43	321.44	290.86	285.24	0.035
O1	-3.03	359.47	321.11	158.52	0.025
O2	-2.71	294.87	286.84	283.01	0.032

Discussion

The vibrational free-energy corrections to E_i and ΔE_{ij} are, respectively, calculated as

$$A_{i,corr}(T) = \sum_i E_i^{ZP} - k_B T \sum_i \ln \left(\frac{1}{1 - \exp\left(\frac{-h\nu_i}{k_B T}\right)} \right)$$

$$\Delta A_{ij,corr}(T) = A_{ij,corr}(T) - A_{i,corr}(T) - A_{j,corr}(T)$$

where ν_i and E_i^{ZP} are, respectively, the vibrational frequency and zero-point energy of the i -th normal mode of the adsorbed O, T is the temperature, and k_B is the Boltzmann constant. In the case of $A_{ij,corr}(T)$, we consider the six vibrational normal modes of the pair of adsorbed O atoms. Results reported in the above table show that the $A_{i,corr}$ values are relatively small, about 1/100 th of the respective E_i values, and uniform across the different sites. The $A_{ij,corr}(T)$ for a pair of O atoms occupying first-neighbor FCC sites was calculated to be 0.075 eV, which produces a free-energy correction of $\Delta A_{ij,corr}(T) = 0.001$ eV to the pair-interaction energy of $\Delta E_{ij} = 0.532$ eV. For a pair of O atoms occupying first-neighbor O2 sites, $\Delta E_{ij} = -0.181$ eV, $A_{ij,corr}(T) = 0.065$ eV, and $\Delta A_{ij,corr}(T) = 0.001$ eV. Therefore, the $\Delta A_{ij,corr}(T)$ values are also relatively small, about 1/100 th of the respective ΔE_{ij} values, and similar for co-adsorption across different pairs of sites. Together, the $A_{i,corr}$ and $\Delta A_{ij,corr}(T)$ values suggest that using adsorption free energies in the Monte Carlo simulations would produce similar thermal distributions of oxygen atoms on Ag(111) as using adsorption (electronic) energies.

Table S4.

(A) Regional coverages of atomic oxygen on Ag(111) at 300 K as a function of total coverage ($\theta_{\text{total}} = 0.125 - 1$ ML) computed using canonical Monte Carlo simulations. (B) Standard deviations for the coverages.

(A)

θ_{total} (ML)	θ_{surf} (ML)	θ_{sub1} (ML)	θ_{sub2} (ML)	$\theta_{\text{near-bulk}}$ (ML)	θ_{bulk} (ML)
0.125	1.250E-01	5.284E-06	0.000E+00	0.000E+00	0.000E+00
0.250	2.499E-01	6.225E-05	0.000E+00	0.000E+00	0.000E+00
0.375	3.739E-01	1.082E-03	0.000E+00	0.000E+00	0.000E+00
0.500	3.923E-01	3.362E-02	7.364E-02	4.080E-04	1.137E-05
0.625	3.870E-01	5.770E-02	1.799E-01	3.421E-04	2.254E-05
0.750	3.769E-01	8.397E-02	2.886E-01	5.340E-04	9.058E-06
0.875	3.678E-01	9.990E-02	4.069E-01	3.170E-04	1.135E-05
1.000	3.547E-01	1.391E-01	4.069E-01	5.714E-04	2.625E-06

(B)

θ_{total} (ML)	θ_{surf} (ML)	θ_{sub1} (ML)	θ_{sub2} (ML)	$\theta_{\text{near-bulk}}$ (ML)	θ_{bulk} (ML)
0.125	7.164E-05	7.164E-05	0.000E+00	0.000E+00	0.000E+00
0.250	2.386E-04	2.386E-04	0.000E+00	0.000E+00	0.000E+00
0.375	1.259E-03	1.259E-03	0.000E+00	0.000E+00	0.000E+00
0.500	1.019E-02	1.171E-02	9.710E-03	1.436E-03	1.053E-04
0.625	8.030E-03	1.226E-02	1.100E-02	5.225E-04	1.497E-04
0.750	7.864E-03	2.456E-02	2.153E-02	7.938E-04	9.392E-05
0.875	7.642E-03	2.234E-02	1.798E-02	5.866E-04	1.052E-04
1.000	4.884E-03	1.865E-02	1.798E-02	9.832E-04	5.060E-05

Table S5.

(A)-(B) Site coverages of atomic oxygen on Ag(111) at 300 K as a function of total coverage ($\theta_{\text{total}} = 0.125 - 1$ ML) computed using canonical Monte Carlo simulations. (C)-(D) Standard deviations for the coverages.

(A)

θ_{total} (ML)	θ_{H} (ML)	θ_{F} (ML)	$\theta_{\text{A+B}}$ (ML)	θ_{O1} (ML)	$\theta_{\text{T1+I1}}$ (ML)
0.125	2.936E-02	9.564E-02	1.034E-07	5.284E-06	0.000E+00
0.250	9.126E-02	1.587E-01	0.000E+00	6.225E-05	0.000E+00
0.375	1.671E-01	2.068E-01	0.000E+00	1.082E-03	0.000E+00
0.500	1.935E-01	1.898E-01	9.020E-03	2.798E-02	5.646E-03
0.625	1.942E-01	1.798E-01	1.302E-02	4.129E-02	1.641E-02
0.750	1.910E-01	1.638E-01	2.206E-02	5.914E-02	2.483E-02
0.875	1.869E-01	1.546E-01	2.632E-02	6.612E-02	3.378E-02
1.000	1.811E-01	1.422E-01	3.137E-02	8.209E-02	5.699E-02

(B)

θ_{total} (ML)	θ_{O2} (ML)	$\theta_{\text{T2+I2}}$ (ML)	θ_{O3} (ML)	$\theta_{\text{T3+I3}}$ (ML)	$\theta_{\text{T+I}}$ (ML)	θ_{o} (ML)
0.125	0.000E+00	0.000E+00	0.000E+00	0.000E+00	0.000E+00	0.000E+00
0.250	0.000E+00	0.000E+00	0.000E+00	0.000E+00	0.000E+00	0.000E+00
0.375	0.000E+00	0.000E+00	0.000E+00	0.000E+00	0.000E+00	0.000E+00
0.500	6.217E-02	1.147E-02	4.331E-07	4.076E-04	1.137E-05	0.000E+00
0.625	1.440E-01	3.585E-02	4.453E-06	3.376E-04	2.254E-05	0.000E+00
0.750	2.350E-01	5.359E-02	4.508E-07	5.336E-04	9.058E-06	0.000E+00
0.875	3.298E-01	7.719E-02	2.268E-06	3.148E-04	1.135E-05	0.000E+00
1.000	3.807E-01	1.249E-01	3.235E-06	5.681E-04	2.625E-06	0.000E+00

(C)

θ_{total} (ML)	θ_{H} (ML)	θ_{F} (ML)	$\theta_{\text{A+B}}$ (ML)	θ_{O1} (ML)	$\theta_{\text{T1+I1}}$ (ML)
0.125	3.422E-03	3.423E-03	1.005E-05	7.164E-05	0.000E+00
0.250	3.652E-03	3.662E-03	0.000E+00	2.386E-04	0.000E+00
0.375	3.333E-03	4.036E-03	0.000E+00	1.259E-03	0.000E+00
0.500	6.359E-03	6.999E-03	3.686E-03	5.620E-03	7.794E-03
0.625	5.840E-03	7.503E-03	4.936E-03	6.085E-03	1.128E-02
0.750	5.828E-03	5.689E-03	6.181E-03	8.853E-03	1.707E-02
0.875	3.844E-03	5.519E-03	4.373E-03	9.571E-03	1.473E-02
1.000	4.520E-03	4.834E-03	5.151E-03	6.291E-03	1.702E-02

Table S5 continued.

(D)

θ_{total} (ML)	θ_{O_2} (ML)	$\theta_{\text{T}_2+\text{I}_2}$ (ML)	θ_{O_3} (ML)	$\theta_{\text{T}_3+\text{I}_3}$ (ML)	$\theta_{\text{T}+\text{I}}$ (ML)	θ_{o} (ML)
0.125	0.000E+00	0.000E+00	0.000E+00	0.000E+00	0.000E+00	0.000E+00
0.250	0.000E+00	0.000E+00	0.000E+00	0.000E+00	0.000E+00	0.000E+00
0.375	0.000E+00	0.000E+00	0.000E+00	0.000E+00	0.000E+00	0.000E+00
0.500	2.468E-02	1.628E-02	2.056E-05	1.436E-03	1.073E-04	0.000E+00
0.625	3.105E-02	2.160E-02	6.580E-05	5.142E-04	1.534E-04	0.000E+00
0.750	5.496E-02	3.420E-02	2.098E-05	7.938E-04	9.362E-05	0.000E+00
0.875	4.706E-02	3.025E-02	4.701E-05	5.860E-04	1.047E-04	0.000E+00
1.000	4.981E-02	3.208E-02	5.611E-05	9.803E-04	5.056E-05	0.000E+00

Table S6.

(A) Regional coverages of atomic oxygen on Ag(111) at 600 K as a function of total coverage ($\theta_{\text{total}} = 0.125 - 1$ ML) computed using canonical Monte Carlo simulations. (B)-(C) Standard deviations for the coverages.

(A)

θ_{total} (ML)	θ_{surf} (ML)	θ_{sub1} (ML)	θ_{sub2} (ML)	$\theta_{\text{near-bulk}}$ (ML)	θ_{bulk} (ML)
0.250	2.491E-01	9.271E-04	3.307E-07	1.851E-07	3.604E-06
0.500	4.055E-01	3.495E-02	5.898E-02	3.154E-04	5.551E-04
0.750	3.830E-01	8.945E-02	2.761E-01	1.211E-03	2.873E-04
1.000	3.580E-01	1.440E-01	4.962E-01	1.631E-03	1.363E-04

(B)

θ_{total} (ML)	θ_{surf} (ML)	θ_{sub1} (ML)	θ_{sub2} (ML)	$\theta_{\text{near-bulk}}$ (ML)	θ_{bulk} (ML)
0.250	9.486E-04	9.472E-04	1.797E-05	1.344E-05	5.931E-05
0.500	9.296E-03	8.407E-03	1.152E-02	6.570E-04	2.873E-04
0.750	7.373E-03	2.318E-02	2.100E-02	1.417E-03	5.344E-04
1.000	8.918E-03	2.979E-02	2.772E-02	1.797E-03	3.609E-04

Table S7.

(A) Regional coverages of atomic oxygen on Ag(111) at $p_{O_2} = 5 \times 10^{-7}$ torr (6.67×10^{-11} bar) as a function of temperature from 300 – 450 K computed using grand-canonical Monte Carlo simulations. (B) Standard deviations for the coverages.

(A)

T (K)	θ_{surf} (ML)	θ_{sub1} (ML)	θ_{sub2} (ML)	$\theta_{near-bulk}$ (ML)	θ_{bulk} (ML)	θ_{total} (ML)
300	4.201E-01	1.273E-02	3.728E-03	1.536E-07	1.755E-06	4.365E-01
325	4.208E-01	7.097E-03	0.000E+00	1.671E-07	0.000E+00	4.279E-01
350	4.205E-01	4.559E-03	0.000E+00	0.000E+00	0.000E+00	4.251E-01
375	4.170E-01	3.359E-03	0.000E+00	0.000E+00	0.000E+00	4.203E-01
400	4.189E-01	1.806E-03	0.000E+00	0.000E+00	0.000E+00	4.207E-01
425	3.905E-01	1.360E-03	0.000E+00	0.000E+00	0.000E+00	3.919E-01
450	1.783E-03	1.215E-07	0.000E+00	0.000E+00	0.000E+00	1.784E-03

(B)

T (K)	θ_{surf} (ML)	θ_{sub1} (ML)	θ_{sub2} (ML)	$\theta_{near-bulk}$ (ML)	θ_{bulk} (ML)	θ_{total} (ML)
300	8.603E-03	3.806E-03	1.141E-02	1.225E-05	4.139E-05	1.479E-02
325	1.008E-02	2.340E-03	0.000E+00	1.277E-05	0.000E+00	1.035E-02
350	1.036E-02	2.079E-03	0.000E+00	0.000E+00	0.000E+00	1.057E-02
375	1.069E-02	1.588E-03	0.000E+00	0.000E+00	0.000E+00	1.081E-02
400	1.355E-02	1.310E-03	0.000E+00	0.000E+00	0.000E+00	1.362E-02
425	2.242E-02	1.002E-03	0.000E+00	0.000E+00	0.000E+00	2.244E-02
450	2.154E-03	1.089E-05	0.000E+00	0.000E+00	0.000E+00	2.154E-03

Table S8.

(A) Regional coverages of atomic oxygen on Ag(111) at $p_{O_2} = 5 \times 10^{-7}$ torr (6.67×10^{-11} bar) as a function of temperature from 425 – 450 K computed using grand-canonical Monte Carlo simulations. (B) Standard deviations for the coverages.

(A)

T (K)	θ_{surf} (ML)	θ_{sub1} (ML)	θ_{sub2} (ML)	$\theta_{near-bulk}$ (ML)	θ_{bulk} (ML)	θ_{total} (ML)
425	3.934E-01	1.196E-03	0.000E+00	0.000E+00	0.000E+00	3.945E-01
430	3.795E-01	8.298E-04	0.000E+00	0.000E+00	0.000E+00	3.803E-01
435	1.946E-01	1.985E-04	0.000E+00	0.000E+00	0.000E+00	1.948E-01
440	3.378E-02	1.554E-06	0.000E+00	0.000E+00	4.346E-09	3.378E-02
445	4.894E-03	2.344E-07	0.000E+00	0.000E+00	0.000E+00	4.895E-03
450	1.831E-03	1.590E-07	0.000E+00	0.000E+00	0.000E+00	1.831E-03

(B)

T (K)	θ_{surf} (ML)	θ_{sub1} (ML)	θ_{sub2} (ML)	$\theta_{near-bulk}$ (ML)	θ_{bulk} (ML)	θ_{total} (ML)
425	2.623E-02	1.106E-03	0.000E+00	0.000E+00	0.000E+00	2.626E-02
430	2.991E-02	9.133E-04	0.000E+00	0.000E+00	0.000E+00	2.992E-02
435	7.566E-02	4.888E-04	0.000E+00	0.000E+00	0.000E+00	7.566E-02
440	1.169E-02	3.892E-05	0.000E+00	0.000E+00	2.060E-06	1.169E-02
445	4.534E-03	1.513E-05	0.000E+00	0.000E+00	0.000E+00	4.534E-03
450	2.202E-03	1.246E-05	0.000E+00	0.000E+00	0.000E+00	2.202E-03

Table S9.

(A) Regional coverages of atomic oxygen on Ag(111) at $p_{O_2} = 0.01$ bar as a function of temperature from 400 – 550 K computed using grand-canonical Monte Carlo simulations.

(B) Standard deviations for the coverages.

(A)

T (K)	θ_{surf} (ML)	θ_{sub1} (ML)	θ_{sub2} (ML)	$\theta_{near-bulk}$ (ML)	θ_{bulk} (ML)	θ_{total} (ML)
400	4.170E-01	4.173E-02	1.841E-01	2.120E-03	1.021E-04	6.451E-01
425	4.219E-01	1.698E-02	2.238E-02	6.421E-05	4.822E-05	4.614E-01
450	4.224E-01	1.049E-02	1.107E-05	1.518E-06	2.529E-05	4.330E-01
475	4.239E-01	7.133E-03	6.743E-06	1.025E-06	2.107E-05	4.310E-01
500	4.240E-01	5.062E-03	5.401E-06	1.167E-06	8.162E-06	4.291E-01
525	4.143E-01	5.647E-03	4.753E-06	1.759E-07	4.905E-06	4.200E-01
550	4.139E-01	4.030E-03	2.765E-06	9.255E-07	8.657E-06	4.179E-01

(B)

T (K)	θ_{surf} (ML)	θ_{sub1} (ML)	θ_{sub2} (ML)	$\theta_{near-bulk}$ (ML)	θ_{bulk} (ML)	θ_{total} (ML)
400	7.549E-03	1.524E-02	7.625E-02	2.880E-03	3.199E-04	7.818E-02
425	1.046E-02	5.166E-03	3.141E-02	2.612E-04	2.167E-04	3.351E-02
450	8.694E-03	3.514E-03	1.035E-04	3.847E-05	1.568E-04	9.380E-03
475	1.023E-02	2.551E-03	8.087E-05	3.162E-05	1.434E-04	1.054E-02
500	1.132E-02	1.857E-03	7.242E-05	3.373E-05	8.921E-05	1.147E-02
525	1.282E-02	2.083E-03	6.796E-05	1.311E-05	6.918E-05	1.299E-02
550	1.464E-02	1.836E-03	5.189E-05	3.005E-05	9.187E-05	1.476E-02

Table S10.

(A) Regional coverages of atomic oxygen on Ag(111) at $p_{O_2} = 0.1$ bar as a function of temperature from 400 – 550 K computed using grand-canonical Monte Carlo simulations.

(B) Standard deviations for the coverages.

(A)

T (K)	θ_{surf} (ML)	θ_{sub1} (ML)	θ_{sub2} (ML)	$\theta_{\text{near-bulk}}$ (ML)	θ_{bulk} (ML)	θ_{total} (ML)
400	4.077E-01	1.114E-01	4.746E-01	3.287E-02	7.598E-04	1.027E+00
425	4.155E-01	4.438E-02	2.194E-01	2.607E-03	1.874E-04	6.821E-01
450	4.176E-01	2.272E-02	5.904E-02	1.589E-04	9.069E-05	4.996E-01
475	4.247E-01	1.113E-02	3.841E-03	3.952E-06	4.266E-05	4.397E-01
500	4.250E-01	8.219E-03	1.503E-05	2.651E-06	4.385E-05	4.332E-01
525	4.228E-01	6.964E-03	9.289E-06	1.590E-06	2.051E-05	4.298E-01
550	4.180E-01	5.605E-03	4.428E-06	1.631E-06	1.502E-05	4.236E-01

(B)

T (K)	θ_{surf} (ML)	θ_{sub1} (ML)	θ_{sub2} (ML)	$\theta_{\text{near-bulk}}$ (ML)	θ_{bulk} (ML)	θ_{total} (ML)
400	8.301E-03	4.629E-02	1.558E-01	2.628E-02	9.640E-04	1.649E-01
425	9.418E-03	1.653E-02	1.068E-01	3.344E-03	4.292E-04	1.085E-01
450	8.612E-03	5.291E-03	3.944E-02	4.734E-04	2.970E-04	4.072E-02
475	9.186E-03	3.499E-03	1.166E-02	6.200E-05	2.034E-04	1.525E-02
500	1.066E-02	2.907E-03	1.208E-04	5.087E-05	2.063E-04	1.105E-02
525	9.826E-03	2.351E-03	9.479E-05	3.937E-05	1.415E-04	1.010E-02
550	1.437E-02	2.297E-03	6.561E-05	3.988E-05	1.210E-04	1.456E-02

Table S11.

(A) Regional coverages of atomic oxygen on Ag(111) at $p_{O_2} = 1$ bar as a function of temperature from 400 – 550 K computed using grand-canonical Monte Carlo simulations.

(B) Standard deviations for the coverages.

(A)

T (K)	θ_{surf} (ML)	θ_{sub1} (ML)	θ_{sub2} (ML)	$\theta_{\text{near-bulk}}$ (ML)	θ_{bulk} (ML)	θ_{total} (ML)
400	3.920E-01	2.379E-01	7.678E-01	3.185E-01	3.142E-02	1.748E+00
425	4.008E-01	1.306E-01	5.901E-01	6.968E-02	2.789E-03	1.194E+00
450	4.137E-01	5.192E-02	2.590E-01	5.390E-03	3.640E-04	7.304E-01
475	4.223E-01	2.268E-02	7.073E-02	2.010E-04	1.897E-04	5.161E-01
500	4.268E-01	1.415E-02	1.485E-02	2.531E-05	1.080E-04	4.559E-01
525	4.231E-01	1.041E-02	3.066E-05	5.255E-06	7.865E-05	4.336E-01
550	4.236E-01	7.432E-03	2.386E-05	5.857E-06	5.236E-05	4.311E-01

(B)

T (K)	θ_{surf} (ML)	θ_{sub1} (ML)	θ_{sub2} (ML)	$\theta_{\text{near-bulk}}$ (ML)	θ_{bulk} (ML)	θ_{total} (ML)
400	1.022E-02	7.986E-02	1.316E-01	2.126E-01	2.545E-02	2.639E-01
425	1.173E-02	5.086E-02	1.735E-01	6.448E-02	4.283E-03	1.924E-01
450	9.147E-03	1.633E-02	9.979E-02	6.040E-03	6.039E-04	1.017E-01
475	9.435E-03	5.843E-03	5.423E-02	5.250E-04	4.279E-04	5.536E-02
500	1.132E-02	4.215E-03	2.355E-02	1.606E-04	3.242E-04	2.647E-02
525	1.178E-02	2.862E-03	1.735E-04	7.145E-05	2.767E-04	1.212E-02
550	1.055E-02	2.713E-03	1.508E-04	7.540E-05	2.257E-04	1.090E-02